CHAPTER 10

CONFIDENCE INTERVALS FOR OCEAN WAVE SPECTRA

Leon E. Borgman

University of Wyoming
Laramie, Wyoming

ABSTRACT

The random nature of ocean wave records introduces statistical variability into the wave spectrum estimates based on these records. This may cause inaccuracy in subsequent calculations such as the prediction of the primary wave direction or the estimation of structural response. Confidence intervals on such estimates are needed to evaluate whether adequate estimate accuracy has been obtained.

The chi-squared confidence interval commonly used for wave spectra is based on the assumption of a Gaussian sea surface. Its applicability for hurrican size waves has been open for question. Therefore, after a brief outline of the relevant statistical relations basic to the chi-squared procedure, wave data from Hurrican Carla is empirically analyzed and compared with the theoretical conclusions. A simulation procedure is used to proceed from the data to probability interval statements. A comparison of these with the correponding chi-squared statements shows the chi-squared relations to be fairly reasonable approximations for spectral estimates averaged over bands of at least eight values. The empirical simulation procedure can be extended to subsequent calculations based on the spectral estimates while the chi-square method encounters difficulty for such problems.

INTRODUCTION

The use of the wave height spectrum to characterize ocean wave conditions is widely used and generally accepted as a very significant mode of analysis for confused sea conditions. If the wave system is unidirectional and produces Gaussian (i.e., multivariate normal) water level elevations, the wave spectrum provides the information for a complete characterization of the statistical properties of the sea surface fluctuations. For a multidirectional wave system, the directional wave spectrum (if it can somehow be estimated accurately) also completely characterizes the statistical properties of the random sea surface provided the sea surface is Gaussian.

The Gaussian assumption is not true for wave systems involving wave heights of appreciable magnitude. It is well known that wave crests typically extend higher above mean water level than the troughs fall below the same level. This would not occur if the sea surface were Gaussian. It has been shown [Pierson, 1955, Brown, 1967, p. 32-37] that the water level elevation in confused sea conditions will be Gaussian if there are no spectral lines present and if linear wave theory holds.

The wave situation of interest to engineers is usually the high sea condition such as occurs in a hurricane. It is very difficult to justify linear wave theory and the Gaussian sea assumption for these circumstances. Nevertheless, the wave spectrum still provides a useful, although not complete, characterization of the statistical properties of the sea surface. Other spectrum-type functions, such as the bispectrum, yield additional information.

Typical wave spectra for hurricanes have been computed and presented by Robinson, Brannon, and Kattawar (1967) and others. These are particularly useful in the study of resonant response and fatigue in engineering structures. They also help give a climatological perspective to the wave conditions which might be encountered. It is expected that as time goes on, more and more engineering design criteria will be tied computationally to the design wave spectrum.

This raises the statistical question of confidence for the spectral estimates. It is desirable to know the approximate accuracy of the estimate. As long as the sea surface was Gaussian and a relatively long record was available for analysis, asymptotic confidence intervals (Blackman and Tukey, 1958, p. 21), based on the chi-squared distribution could be used. This procedure is no longer strictly applicable for the nonlinear wave conditions in a hurricane. What should be used then? For that matter, what are the statistical properties of the wave spectrum values for hurricane conditions? These questions will be examined in detail.

WAVE SPECTRUM ESTIMATION

Two basic procedures have been used for estimating the wave spectrum. The first of these (Blackman and Tukey, 1958) is based on using the data to estimate the covariance function and then numerically making the cosine Fourier transform of the covariance function to get the raw wave spectrum. The second method (Bingham, Godfrey, and Tukey, 1967) uses the "fast Fourier transform" computer algorithm to get the raw wave spectrum directly from the data.

The word "raw" in the above paragraph refer to the spectrum before it is smoothed or modified in various ways to improve the statistical properties of the spectrum estimate. Both basic procedures give the same general results, if the modifications could be deleted. This is difficult for the covariance method since the estimation of the covariance intrinsically causes an equivalent spectral smoothing.

From the viewpoint of simplicity, computational speed, and the preservation of information, the fast Fourier transform procedure is preferrable. Therefore it will be the method used in the following analysis. The fast Fourier transform (here after designated FFT) is a computer algorithm for rapidly computing

$$A_m = \Delta t \sum_{n=o}^{N-1} \eta_n \exp(-i2\pi mn/N) \qquad (1)$$

or its inverse

$$\eta_n = \Delta f \sum_{m=o}^{N-1} A_m \exp(i2\pi mn/N) \qquad (2)$$

Here Δt represents a time increment and Δf is a frequency increment. This notation is used since with it the FFT is directly and obviously the finite difference approximation to the integral Fourier transform. In order for equations (1) and (2) to be exact inverses of each other, Δt and Δf must satisfy

$$(\Delta t)\ (\Delta f) = 1/N \tag{3}$$

The significance of relations (1) and (2) for wave analysis can be seen if η_n (n=0, 1, 2, ..., N-1) is taken to be water level elevations above mean water level from a wave recorder digitzed at Δt increment apart. Then is real-valued and (2) reduces to

$$\eta_n = \Delta f \sum_{m=o}^{N-1} [U_m \cos(2\pi mn/N) + V_m \sin(2\pi mn/N)] \tag{4}$$

$$= \Delta f \sum_{m=0}^{N-1} \sqrt{U_m^2 + V_m^2}\ \cos\left(2\pi \frac{mn}{N} - \phi_m\right) \tag{5}$$

where

$$A_m = U_m - iV_m$$

and

$$\phi_m = \arctan(V_m/U_m)$$

Thus, computation of A_m provides the coefficients for a trigonometric series representation of the wave record. The mean-square fluctuation (variance) attributable to the m-th senusoid is (with $n/N = n\Delta t/N\Delta t = t/T$)

$$\text{mean-square} = \frac{1}{T}\int_0^T [\Delta f \sqrt{U_m^2 + V_m^2}\ \cos(2\pi mt/T - \phi_m)]^2\, dt$$

$$= \frac{(\Delta f)^2}{T}\int_0^T (U_m^2 + V_m^2)\ [1/2 + 1/2 \cos 2\ (2\pi mt/T - \phi_m)]\, dt$$

$$= (\Delta f)\ (U_m^2 + V_m^2)/\ (2T) \tag{6}$$

Here, the relation (3) together with $T = N\Delta t$ has been used to obtain $\Delta f = 1/T$ The variance per unit frequency or spectral density is, thus,

$$\frac{\text{mean-square}}{\Delta f} = \frac{U_m^2 + V_m^2}{2T} = \frac{|A_m|^2}{2T} \tag{7}$$

It follows from (1) that $|A_{N-m}|^2 = |A_m|^2$. Hence it is only necessary to list the expression in (7) for m = 0, 1, 2, ..., N/2 since from there on the values are mirror images of the preceding ones. The frequency, $N\Delta f/2$, corresponding to m = N/2 is called the Nyquist freqency. It is a useful convention to tabulate double the expression in (7) versus m = 0, 1, 2, ..., N/2 so that $|A_m|^2/T$ gives the variance for the m-th and the (N-m)-th terms combined. Hence raw spectral density estimates are defined as

$$S_m^* = |A_m|^2/T \tag{8}$$

THEORETICAL STATISTICAL PROPERTIES

Because the chi-squared confidence interval for the wave spectrum is so often used blindly without an appreciation of the applicability of the method to that particular wave data, the theoretical basis for the chi-squared confidence interval will be outlined in some detail.

If the sequence of sea surface elevations $\{\eta_n, n= 0, 1, 2, ..., N-1\}$ are regarded as a random vector with intercorrelated components, a number of results can be derived for the real and imaginary parts of A_m. It will be assumed that the stochastic sequence is second-order stationary and η_n has zero expectation. The theoretical covariance sequence and spectral density will be defined as

$$C_k = E[\eta_n \eta_{n+k}] \tag{9}$$

$$S_m = \Delta t \sum_{k=0}^{N-1} C_k \exp(-i2\pi mk/N) \tag{10}$$

The expression $E[\cdot]$ denotes the expectation operator (Freund, 1962, Chapter 4, p. 90).

From the above frame work, it is possible to derive a number of statistical properties for

$$U_m = \Delta t \sum_{n=o}^{N-1} \eta_n \cos(2\pi mn/N) \tag{11}$$

$$V_m = \Delta t \sum_{n=o}^{N-1} \eta_n \sin(2\pi mn/N) \tag{12}$$

It can be shown that (1) U_m and V_m have zero expectations, (2) U_m and V_m are asymptotically independent, (3) the components of the vectors (U_m, V_m) and $(U_{m'}, V_{m'})$ are asymptotically independent of each other, and (4) the variances of U_m and V_m, for $0<m<\frac{N}{2}$ are the same and equal to $TS_m/2$. The word "asymptotic in the above results refers to N approaching infinity while the covariance sequence is zero for k larger than some fixed integer.

Asmptotically, then,

$$E[S_m^*] = E\left[\frac{U_m^2 + V_m^2}{T}\right] = \frac{Var(U_m) + Var(V_m)}{T}$$

$$= \frac{1}{T}\left(\frac{TS_m}{2} + \frac{TS_m}{2}\right) = S_m \qquad (13)$$

and S_m^* is asymptotically unbiased as an estimate of S_m.

If, in addition to the above assumptions, $\{\eta_n,\ n = 0, 1, 2, \ldots, N-1\}$ is a multivariate normal vector it follows that $(U_m, V_m, U_{m'}, V_{m'})$ is also a multivariate normal random vector. This is true since any linear transformation of a normal vector is again normal (Lindgren, 1960, p. 129) and equations (11) and (12) show that U_m and V_m are linear combinations of the η_n. Hence $U_m/\sqrt{TS_m/2}$ and $V_m/\sqrt{TS_m/2}$ are standard normal random variables and, as mentioned above, asymptotically independent. The sum of the squares of two independent standard normal random variables is a chi-square random variable with 2 degrees of freedom (Freund, 1962, p. 194). Thus

$$\frac{S_m^*}{S_m} = \frac{U_m^2 + V_m^2}{TS_m} = \tfrac{1}{2}\left[\left(\frac{U_m}{\sqrt{TS_m/2}}\right)^2 + \left(\frac{V_m}{\sqrt{TS_m/2}}\right)^2\right] = \frac{\chi_2^2}{2} \qquad (14)$$

(asymptotically)

Now suppose $\hat{S}_{m_o}$ is the average of b values of S_m^* and that S_m is constant over the b values. Then asymptotically

$$\hat{S}_{m_o} / S_{m_o} = \frac{1}{b}\sum_{j=r}^{b+r}(S_m^* / S_m) = \frac{\chi_{2b}^2}{2b} \qquad (15)$$

where r is the first in value in the band and m_o is the mid frequency of the band. Equation (15) holds since the sum of independent chi-squares is again a chi-squared random variable with degrees of freedom equal to the sum of the degrees of freedom of the individual summands (Freund, 1962, p. 194).

The relation (15) is the basis for the chi-squared confidence interval used so often for wave spectra.

$$P\left[\frac{2b\hat{S}_m}{\chi^2_{2b,\,1-\frac{\alpha}{2}}} < S_m < \frac{2b\,\hat{S}_m}{\chi^2_{2b,\,\frac{\alpha}{2}}}\right] = 1-\alpha \qquad (16)$$

In the above expression, $\chi^2_{2b,c}$ refers to the c-th percentile of a chi-squared variate with 2b degrees of freedom.

What then should the user beware of relative to the chi-square confidence interval for wave spectra? Some of the points to consider are as follows. (a) the Length of record analyzed (i.e., the value of N) should be as large as possible consistent with avoiding non-stationary conditions. For most wave situations, a commonly used choice is 20 mintes of record. (b) the covariance function should be essentially zero for lags substantially less than the wave record length. One published suggestion is that the maximum covar-

iance lag with appreciable non-zero covariance values should be on the order of one-tenth of the record length (Blackman and Tukey, 1958, p. 11). (c) The closer the wave conditions come to satisfying linear wave theory, the better will be the confidence interval approximation provided by (16), and vice-versa.

EMPIRICAL DATA ANALYSIS

Wave data from hurricane Carla was selected to test the accuracy of the chi-squared confidence interval under extreme conditions. Water level elevations (4096 values) digitized at an inverval of 0.2 seconds apart and starting at noon, September 8, 1961 were used. The wave records were made in 100-ft. water depth by the Chevron Research Company on a Chevron platform in South Timbaker Block 63, Gulf of Mexico, as a part of their Wave Project II (Thrasher and Aagaard, 1970) and have been released to the National Oceanographic Data Center. The FFT coefficient, A_m, were computed by the NLØGN subroutine (Robinson, 1967, p. 63) and S_m^* was tabulated for $m = 0, 1, 2, \ldots, 4095$. The values of S_m^* for $6 < m < 305$ were selected by inspection as being significantly different from zero. These values, graphed in Fig. 1 versus $f = m\Delta f$, are the basic initial information from which the wave spectrum is estimated.

The scattered points must be averaged in some manner to produce a mean curve. Fig. 2 shows the results of two different averaging methods. The dashed line gives the results of straight arithmetic averaging in blocks of 8 lines. The solid line gives the spectrum as determined from the following weighted average

$$S_m^* = \left[\sum_j W_{m-j} S_j^* \right] / \left[\sum_j W_{m-j} \right] \tag{17}$$

where

$$W_{m-j} = e^{-[(m-j)\Delta f]^2 / (2\sigma^2)} \tag{18}$$

$$\sigma = 3\Delta f$$

This averaging will be referred to as Gaussian smoothing because of the analogy to the normal or Gaussian density. The two spectral estimates are almost identical. The Gaussian smoothing was selected as preferrable for the present study because it gives the greatest emphasis in averaging to nearby points and the least emphasis to points further away. This is different from the block averaging which equally weights points within the block.

The scatter of the raw spectrum points about the Gaussian-smoothed spectrum estimate was examined next. The residuals, or deviations of S_m^* from the spectrum estimate

$$R_m = \hat{S}_m - S_m^*$$

are plotted at the bottom of Fig. 3. As would be expected the residuals are the biggest for frequencies where the spectrum is large. The magnitude of the residuals at different frequencies was characterized by three different root-mean-square values. These were

$$\begin{aligned} \sigma_m &= \text{r.m.s. } R_m \\ \sigma_{m+} &= \text{r.m.s. positive } R_m \\ \sigma_{m-} &= \text{r.m.s. negative } R_n \end{aligned} \tag{19}$$

The first formula uses (17) and (18) as written except R_j^2 is substituted for S_j^*. The second formula applies (17) and (18) only to the R_j^2 where R_j is greater than zero. The third formula does the same for the negative R_j. All three Gaussian averages are then square-rooted to get the root-mean-square values. The quantities σ_{m+}, and σ_{m-} are graphed versus frequency in Fig. 4. Although computed, σ_m is not shown since it did not prove to be useful in later parts of the study.

As Fig. 4 shows, σ_+ has a much larger maximum than σ_-. Also both maxima more or less coincide with the peak of the spectral density.

The residuals were first normed by dividing them by σ_m. These values are graphed as the normed residuals shown in Fig. 3. Originally it was intended to use these normed residuals as the stationary noise characterization of the spectrum deviations. However a careful examination of the normed residuals shows that their minimum values are larger around 0.10-0.15 Hertz than elsewhere. Thus the noise in this form does not appear to be stationary.

The residuals were then normed by dividing positive R_m by σ_{m+} and dividing negative R_m by σ_{m-}. These symmetrically normed residuals are plotted at the top of Fig. 3. A Smirnov k-sample test applied to six groups of 50 each of these (Conover, 1971, p. 322) leads to an acceptance that the noise represented by the symmetrically normed residuals is essentially stationary (See Fig. 6). Thos noise was therefore used to characterize the fluctuations about $\hat{S}_m$.

The empirical distribution function of the symmetrically normed residuals is shown as the solid line in Fig. 7. The corresponding probability density function was estimated from the slope of the straight line fitted by least squares to the empirical distribution function using the values in a band of width $\pm$ 0.5 about the abscissa value for which the density is being estimated. A graph of the density is given in Fig. 8.

A COMPARISON WITH THEORY

How do the above empirical results compare with the theory outlined previously? Theoretically, the S_m^* are supposed to be asymptotically independent. This would imply that the symmetrically normed residuals would also be independent. This would imply that the symmetrically normed residuals would also be independent. As a partial test of this property, the m-th symmetrically normed residual was graphed versus the (m+1)-th corresponding value as

shown in Fig. 5. The scatter shows no clear cut trend except for a tendency to produce a square cloud of points. The squareness is explained by the abrupt start and termination of the density function in Fig. 8. If the density were uniform, for example, and the residuals independent a perfectly square cloud would be expected. Thus, Fig. 5 does not appear to contradict the asymptotic independence.

The chi-square distribution with two degrees of freedom which theoretically should approximately hold for S_m^* was checked next. Symmetrically norming a χ_2^2 random variable produces a variable with a distribution function shown by the dash-dot curve in Fig. 7. The corresponding theoretical density function is graphed in Fig. 8. The discontinuity results from the abrupt change in norming constant at zero.

A Kolmogarov test for goodness-of-fit at the .05 level can be performed by inspection of Fig. 7. The distribution function for the symmetrically normed χ_2^2 variate passes outside the 90% Kolmogorov confidence band (Conover, 1971, p. 299) and therefore causes a rejection of the hypothesis that the data follow that theoretical distribution.

Despite this rejection, it is interesting to compare the chi-squared probability predictions with what would follow from the symmetrically normed noise. By Monte-Carlo procedures, independent noise having the empirical distribution function given in Fig. 7 was assigned at random to the different m values. Then σ_+, σ_-, and $\hat{S}_m$ were used to reconstruct the S_m^* values consistent with this noise. Finally a new set of $\hat{S}_m$ values were computed by Gaussian smoothing. These $\hat{S}_m$ values would be an equivalent possibility to that which actually occurred if the noise had just been shifted around to an equally likely realization. Three hundred such sets of $\hat{S}_m$ values were developed and 90% probability intervals were established from the 5th and 95th percentiles of simulated values. These are shown in Fig. 9.

The Gaussian smoother used in deriving the original $\hat{S}_m$, had a width roughly equivalent to band of 8 spectral lines.(Its standard deviation was 3 lines and the width is somewhat larger than $\pm\sigma$.) Hence it seems reasonable to compare the probability intervals with that for a chi-squared with b = 8, or 2b = 16. This is shown in Fig. 10. The two probability interval sets are slightly but not terribly different. One would have to conclude that the chi-squared approximation is reasonably adequate, even for hurricane waves. This seems true despite the disagreement relative to the S_m^* values. Something like a central limit theorem seems to be pulling the distributions into agreement for averages of bands including as many as 8 raw spectral values.

ADDITIONAL DOCUMENTATION PLANNED

Empirical Analysis has continued on the Hurrican Carla data. About half of the available data sets have been analyzed. The empirical distribution functions and probability densities for these (seven more records) are all remarkably identical with Figs. 7 and 8. The Smirnov k-sample test overwhelmingly accepts that they all have the same distribution function. It is planned that the detailed empirical analysis of the Hurricane Carla spectra and of a variety of spectra for other wave conditions will be issued as a project report as soon as the analysis is complete.

CONCLUSIONS

The available data supports the use of the chi-squared approximation for a confidence interval on spectrum estimates. It is difficult however to extend the chi-squared approximation to yield confidence intervals on subsequent quantities computed from wave spectra. For such situations, simulation procedures based on the empirical properties of the spectral noise would seem to provide a reasonable approach to developing confidence intervals.

ACKNOWLEDGEMENTS

This investigation was supported by Contract DACW72-72-C-0001 with the Coastal Engineering Research Center, Corps of Engineers, U.S. Army. Appreciation is expressed to Mr. Richard Whitaker and Mr. Jack Wolff, graduate students at the University of Wyoming, for their assistance in computer calculations.

REFERENCES

Bingham, C., Godfrey, M. D., and Tukey, J. W. (1967), "Modern Techniques of Power Spectrum Estimation" IEEE Trans. Audio and Electroacoustics, vol. AU-15, no. 2, pp. 56-66.

Blackman, R. B., and Tukey, J. W. (1959), "The Measurement of Power Spectra," Dover, New York.

Brown, L. J. (1967), "Methods for the Analysis of Non-stationary Time Series with Applications to Oceanography," Hydraul. Eng. Lab. Rep. HEL 16-3, College of Eng., University of California, Berkeley.

Conover, W. J., (1971), "Practical Nonparametric Statistics," John Wiley and Sons, Inc., New York.

Freund, J. E., (1962), "Mathematical Statistics," Prentice-Hall, Inc., Englewood Cliffs, New Jersey.

Lindgren, B. W., (1960), "Statistical Theory," Macmillan Co., New York.

Pierson, W. J., Jr., (1955) "Wind-Generated Gravity Waves," Advances in Geophysics, vol. 2, pp. 93-178.

Robinson, E. A., (1967), "Multichannel Time Series Analysis with Digital Computer Programs," Holden-Day, San Francisco.

Robinson, R. J., Brannon, H. R., and Kattawar, G. W., (1967), "Storm Wave Characteristics," Trans. Soc. of Petroleum Eng. of AIME, vol. 240, pp. 87-98.

Thrasher, L. W., and Aagaard, P. M., (1970), "Measured Wave Force Data on Offshore Platforms," Jour. Petroleum Technology, vol. 22, pp. 339-346.

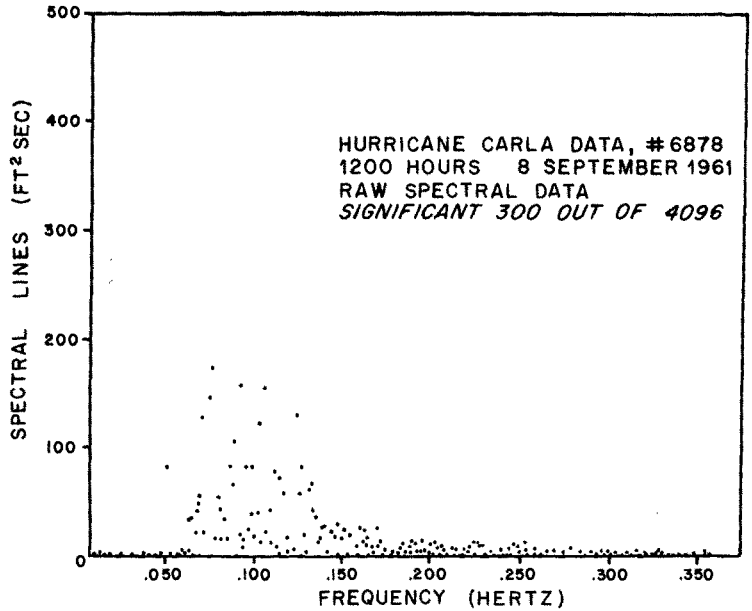

Fig. 1. Values of S_m^* versus $m\Delta f$

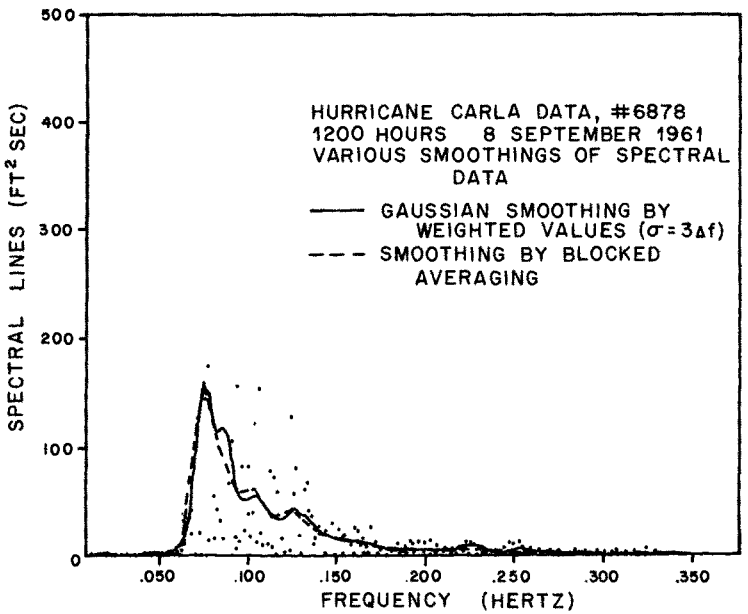

Fig. 2. The spectrum estimate $\hat{S}_m$ determined by two different methods.

Fig. 3. Various versions of residuals plotted versus frequency.

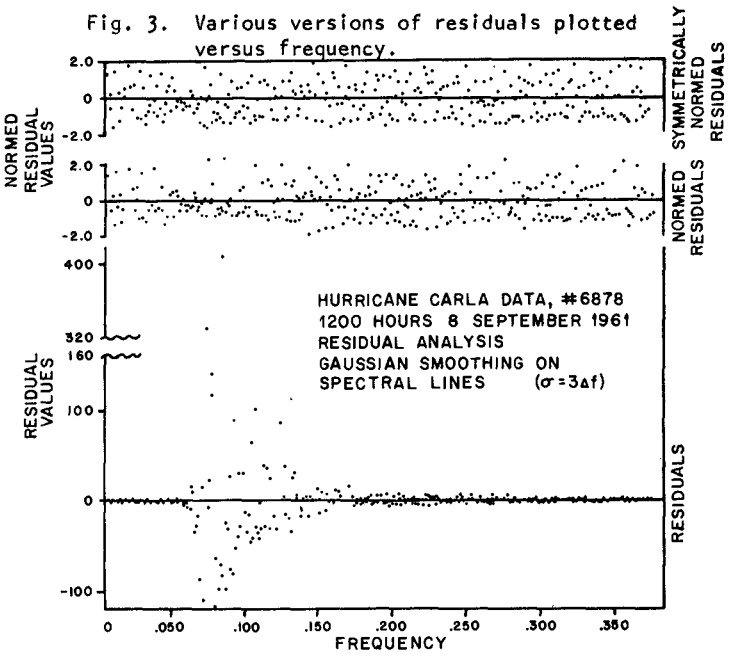

Fig. 4. Local estimates of standard deviation.

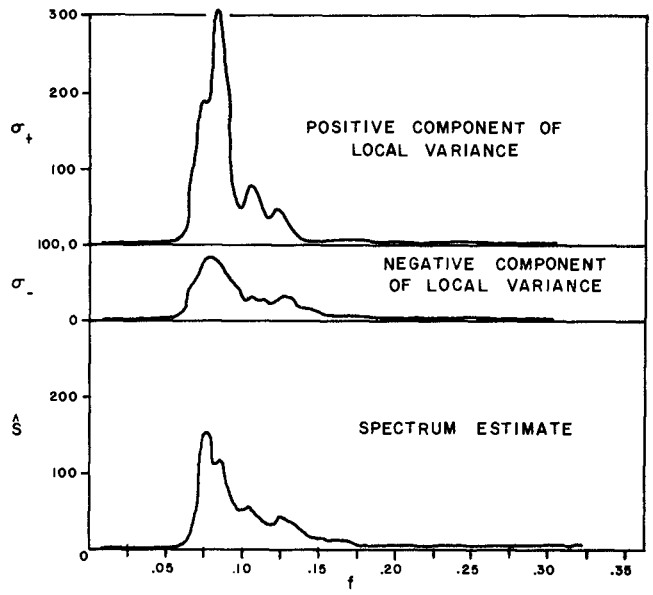

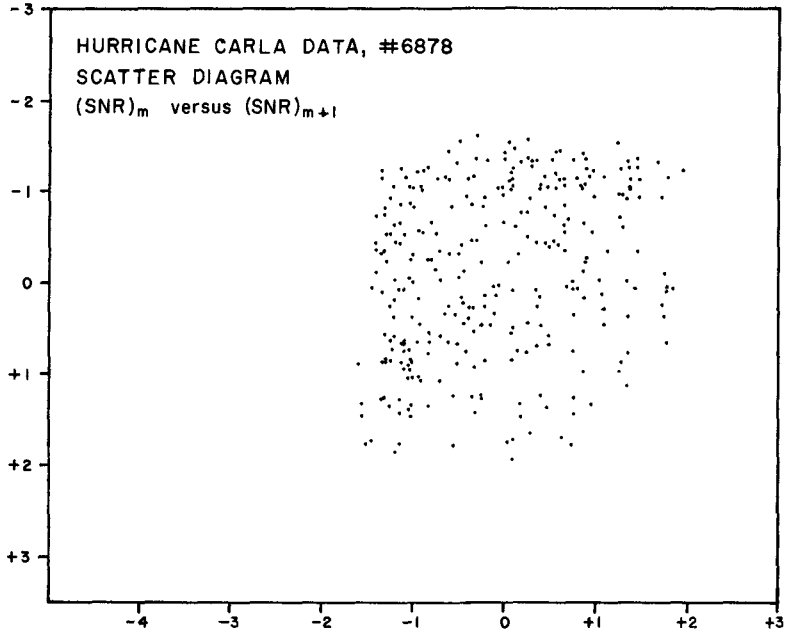

Fig. 5. Scatter diagram of the m-th symmetrically normed residual plotted versus the (m+1)-th value.

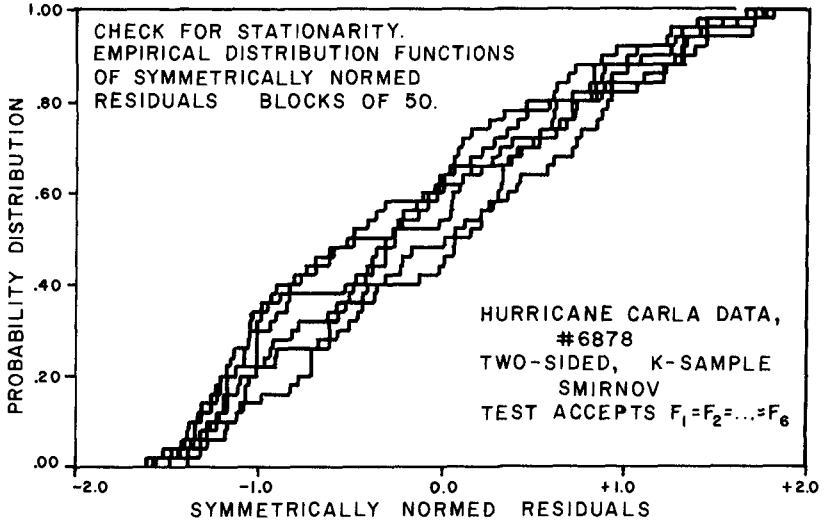

Fig. 6. Smirnov test of noise stationarity.

Fig. 7. The empirical distribution function of the noise as compared with a symmetrically normed chi-square distribution function.

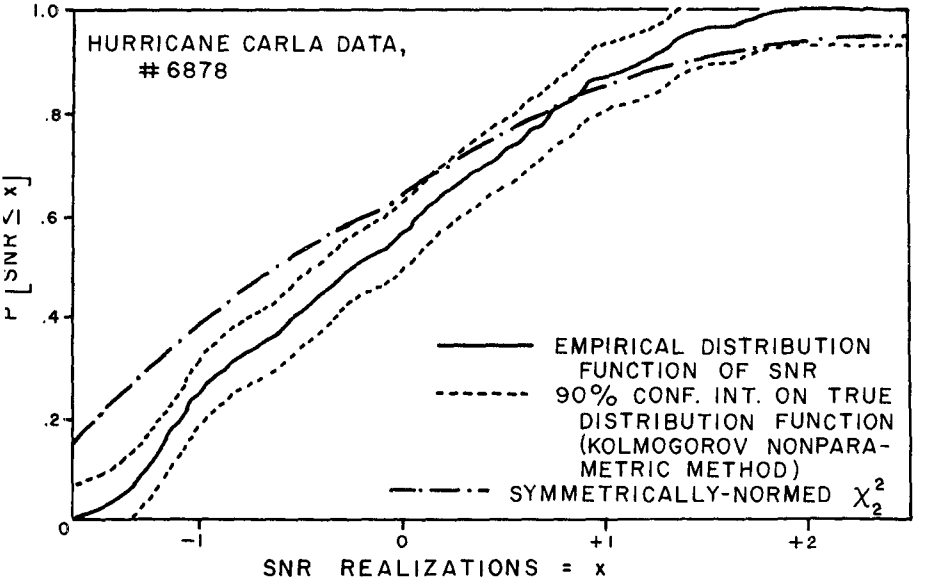

Fig. 8. Probability densities for the noise and a symmetrically normed chi-squared random variable.

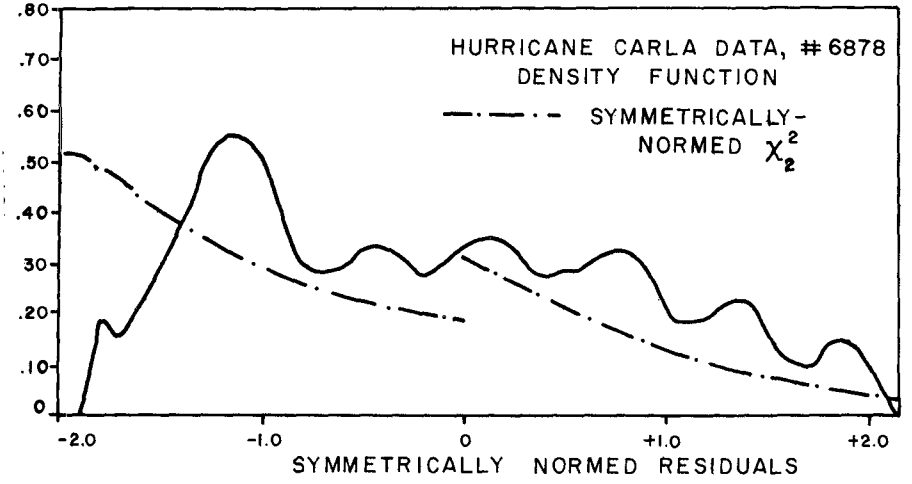

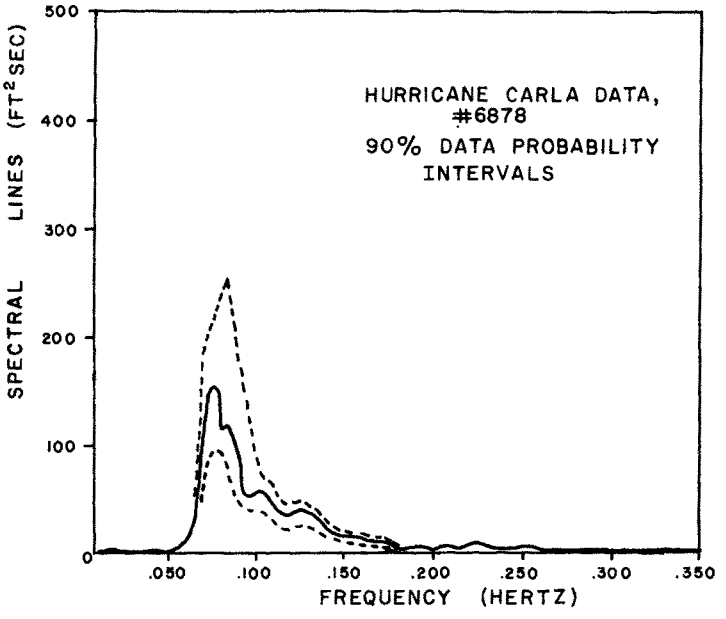

Fig. 9. Empirical probability intervals as determined from simulation.

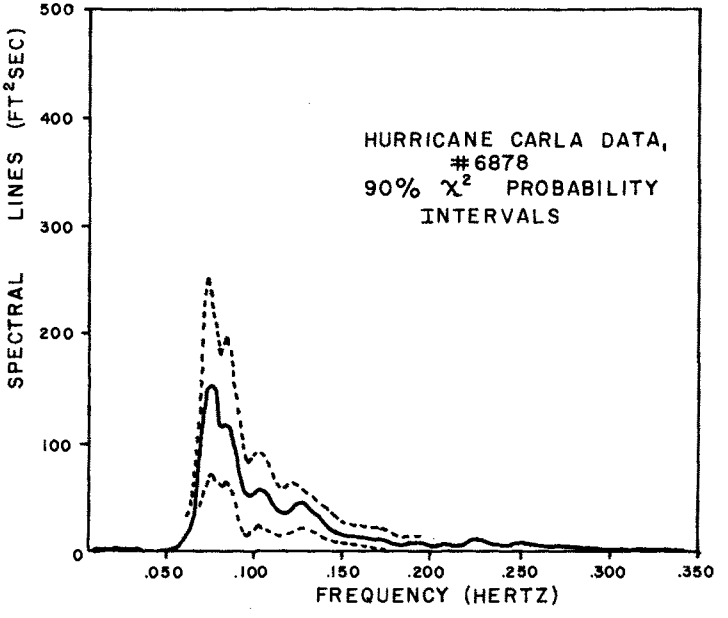

Fig. 10. Chi-square probability intervals (16 degrees of freedom).